

# Ocean heat uptake efficiency increase since 1970

B. B. Cael<sup>1</sup>

<sup>1</sup>National Oceanography Centre, Southampton, UK.

This is a non-peer reviewed preprint submitted to EarthArXiv; this manuscript is in review at *Geophysical Research Letters*.

## Key Points:

- Ocean heat uptake efficiency (OHUE) change is estimated from ocean heat content and global mean surface temperature records.
- There is a >99% probability that ocean heat uptake efficiency increased over the past five decades.
- OHUE was on average  $0.58 \pm 0.08$  W/m<sup>2</sup>K over this period and increased during it by  $0.19 \pm 0.04$  W/m<sup>2</sup>K.

---

Corresponding author: B. B. Cael, [cael1@noc.ac.uk](mailto:cael1@noc.ac.uk)

**Abstract**

The ocean stores the bulk of anthropogenic heat in the Earth system. The ocean heat uptake efficiency (OHUE) – the flux of heat into the ocean per degree of global warming – is therefore a key factor in how much warming will occur in the coming decades. In climate models, OHUE is well-characterised, tending to decrease on centennial timescales; in contrast, OHUE is not well-constrained from Earth observations. Here OHUE and its rate of change are diagnosed from global temperature and ocean heat content records. OHUE increased over the past five decades by  $0.19 \pm 0.04$  W/m<sup>2</sup>K, and was on average  $0.58 \pm 0.08$  W/m<sup>2</sup>K during this period. This increase is attributed to steepening anthropogenic heat gradients in the ocean, and corresponds to several years’ difference in when temperature targets such as 1.5°C or 2°C are exceeded.

**Plain Language Summary**

Human activity causes extra energy to be radiated back onto Earth’s surface. Much of this extra energy accumulates in the ocean as heat. Based on records of global warming and the ocean’s heat content, here it is shown that the *efficiency* of the transfer of this energy into the ocean has increased in recent decades. This ‘ocean heat uptake efficiency’ is the amount of energy transferred into the ocean per degree of global warming, and has increased by roughly a third over the past five decades. This translates into several years’ delay until global warming temperature targets, such as 2°C warming, are exceeded.

**1 Introduction**

Global warming can be understood in terms of conservation of energy of the Earth’s surface. The amount of warming corresponds to the difference between the extra energy radiated to the Earth’s surface via anthropogenic and natural factors, i.e. the radiative forcing, versus the amount of that energy that is exported elsewhere (Sellers, 1969). A key reservoir for the export of this excess energy is the ocean, which contains almost all of the anthropogenic heat in the Earth system (Cheng et al., 2017; Levitus et al., 2012; Domingues et al., 2008; JMA, 2022; Cheng, 2022). This ocean heat content (OHC  $\mathcal{H}$ , [ZJ = 10<sup>21</sup>J]) has increased by hundreds of zetajoules over the past several decades of sustained ocean observations, during which time Earth’s global mean surface temperature anomaly ( $T$ , [K]) has increased by about 1°C (Morice et al., 2021; Hersbach et al., 2020; Rohde & Hausfather, 2020; Cowtan & Way, 2014; Hansen et al., 2006; Lindsey & Dahlman, 2020).

More important than OHC for future climate change is the ocean heat uptake *efficiency* (OHUE,  $\kappa$  [W/m<sup>2</sup>K], Materials and Methods (MM)) (Gregory & Mitchell, 1997; Newsom et al., 2020), that is, how much energy Earth’s surface exports downwards into the ocean per degree of global warming.  $\kappa$  is thus an integrated metric of the climate system’s capacity to ‘resist’ surface warming by fluxing excess energy (i.e. anthropogenic heat) into the ocean, and is determined by numerous factors including the surface pattern of warming (Newsom et al., 2020; Armour et al., 2013; Rose et al., 2014) and the ocean circulation (Gregory et al., 2015; Winton et al., 2010; Watanabe et al., 2013). The impact of OHUE on global warming is most simply expressed via a metric sometimes referred to as the transient climate sensitivity (TCS [K], MM) (Padilla et al., 2011; Winton et al., 2010; Raper et al., 2002), which expresses the expected warming at the time that the atmospheric CO<sub>2</sub> concentration reaches double its pre-industrial level after decades of sustained anthropogenic emissions. TCS is defined as  $TCS = F_{2xCO_2} / (-\lambda + \kappa)$ , where  $F_{2xCO_2}$  [W/m<sup>2</sup>] is the radiative forcing associated with a doubling of the atmospheric CO<sub>2</sub> concentration from pre-industrial levels and  $\lambda$  [W/m<sup>2</sup>K] is the climate feedback, which analogous to  $\kappa$  corresponds to how much energy Earth’s surface exports upwards to space per degree of global warming (Sherwood et al., 2020) (n.b. the sign conventions

of  $\kappa$  and  $\lambda$  are such that a negative (positive)  $\lambda$  ( $\kappa$ ) stabilises the climate). The larger the value of  $\kappa$ , the less warming is expected in coming decades.

OHUE is fairly well-characterised within Earth System Models (ESMs, including coupled atmosphere-ocean general circulation models). This is mostly via experiments where atmospheric  $\text{CO}_2$  is increased by 1% per year for 70 years, after which time it has doubled; OHUE can then be defined as the ratio of  $\mathcal{H}$  and  $T$  after about 70 years, for instance (Gregory & Mitchell, 1997; Kuhlbrodt & Gregory, 2012). Notably, when these experiments are run for 140 years to the point that that atmospheric  $\text{CO}_2$  quadruples, OHUE almost always decreases between  $\sim 70$  and  $\sim 140$  years, though by how much varies substantially between models (Gregory et al., 2015; Watanabe et al., 2013). While these scenarios are of limited use for describing real historical climatic changes, they are a core component of idealised understanding of OHUE.

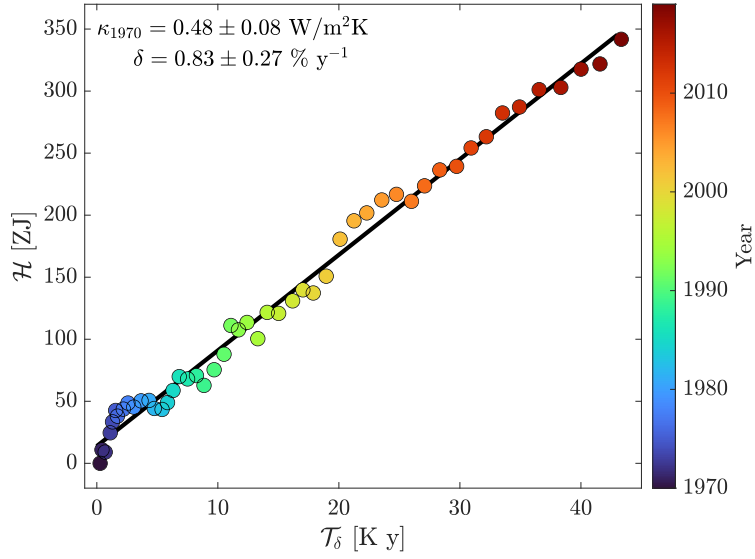
In contrast, OHUE is poorly constrained for the real climate system, hindering efforts to validate ESMs' predictions of climate change in coming decades. Here a method is presented to diagnose OHUE from observations of ocean heat content and temperature alone (MM). OHUE significantly increased by  $0.19 \pm 0.04 \text{ W/m}^2\text{K}$  over the past five decades ( $>99\%$  confidence). This is attributed to the steepening of anthropogenic heat gradients in the ocean, rather than ocean circulation changes, and corresponds to several years' delay in when the temperature targets laid out in the Paris Agreement are exceeded (*Adoption of the Paris Agreement FCCC/CP/2015/L.9/Rev.1*, 2015).

## 2 Results and Discussion

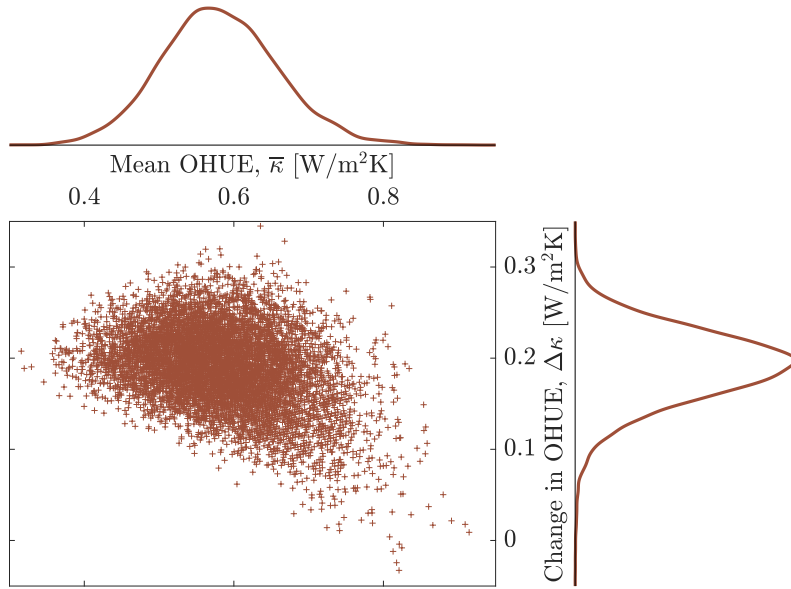
The method is described in detail in MM. Briefly, the OHC ( $\mathcal{H}$ ) is regressed against the integral of the time-weighted temperature anomaly  $\mathcal{T}$ ; the slope of this regression corresponds to  $\kappa$ . An ensemble derived from the infilled HadCRUT5 (Morice et al., 2021) ensemble experiment is used for  $T$ , and an ensemble derived from the JMA (JMA, 2022; Ishii et al., 2017), Cheng (Cheng et al., 2017; Cheng, 2022), and NCEI (Domingues et al., 2008; Levitus et al., 2012)  $\mathcal{H}$  products is used for  $\mathcal{H}$  (MM). The years 1970-2019 are used because these are the years with enough signal relative to measurement uncertainties (MM). There is significant (probability  $>99\%$ ) positive curvature in the residuals of this regression (MM), indicating a time-evolution of  $\kappa$ . This is captured by an ansatz that  $\kappa$  changes linearly with time, from an initial value  $\kappa_{1970} [\text{W/m}^2\text{K}]$ , by a fixed amount  $\delta\kappa_{1970} [\text{W/m}^2\text{Ky}]$  each year. This ansatz is introduced by replacing  $\mathcal{T}$  with an integrated time-weighted temperature anomaly  $\mathcal{T}_\delta$ ; the best-fitting  $\delta$  value for each temperature ensemble member is selected with its corresponding  $\kappa_{1970}$  to quantify uncertainty. The ansatz is then verified by the absence of curvature in the residuals of  $\mathcal{H}$  regressed against  $\mathcal{T}_\delta$  (Figure 1). Thus, both the time-mean OHUE from the 1970s through the 2010s and the time evolution of OHUE, as approximated by a linear trend, are captured.

Figure 2 shows the joint distribution of the time-average OHUE, i.e. the mean of  $\kappa$ , and the change in  $\kappa$ , i.e. the final minus initial  $\kappa$  value, over this period. It is found with  $>99\%$  probability that OHUE increased (i.e.  $\delta > 0$ ) over the past five decades and that this increase is well-described as increasing with time rather than being a temperature-dependent effect (MM). The uncertainty in these two quantities is anticorrelated (Figure 2), such that the uncertainty in  $\kappa$  reduces slightly over time.

This trend corresponds to a fairly large relative change of  $34 \pm 9\%$  in OHUE over the past five decades (Figure 3). This trend corresponds to an additional  $113 \pm 35 \text{ ZJ}$  of heat stored in the ocean during this time period versus if OHUE stayed at its initial 1970 value, which is enough to heat the top  $\sim 45\text{m}$  of the ocean by  $1^\circ\text{C}$ , and  $29 \pm 9\%$  of the total OHC accumulated during this time period. This trend also has appreciable consequences for near-term warming. Using standard values of  $F_{2x\text{CO}_2} = 4 \pm 0.3 \text{ W/m}^2$  and  $\lambda = -1.3 \pm 0.44 \text{ W/m}^2\text{K}$  (Sherwood et al., 2020), under a scenario where atmo-



**Figure 1.** Illustration of regression of ocean heat content ( $\mathcal{H}$ , [ZJ], ensemble median shown) vs. weighted temperature integral ( $\mathcal{T}_\delta$ , [K y], ensemble median shown) to find initial ocean heat uptake efficiency ( $\kappa_{1970}$ , [ $\text{W/m}^2\text{K}$ ]) and rate of change ( $\delta$ , [ $\text{y}^{-1}$ ]).



**Figure 2.** Joint distribution of time-mean ocean heat uptake efficiency ( $\bar{\kappa}$ , [ $\text{W/m}^2\text{K}$ ]) and change in ocean heat uptake efficiency ( $\Delta\kappa$ , [ $\text{W/m}^2\text{K}$ ]) from 1970-2019. Y-axes of top and right-hand side plots are probability densities with units the inverse of those on the corresponding X-axes.

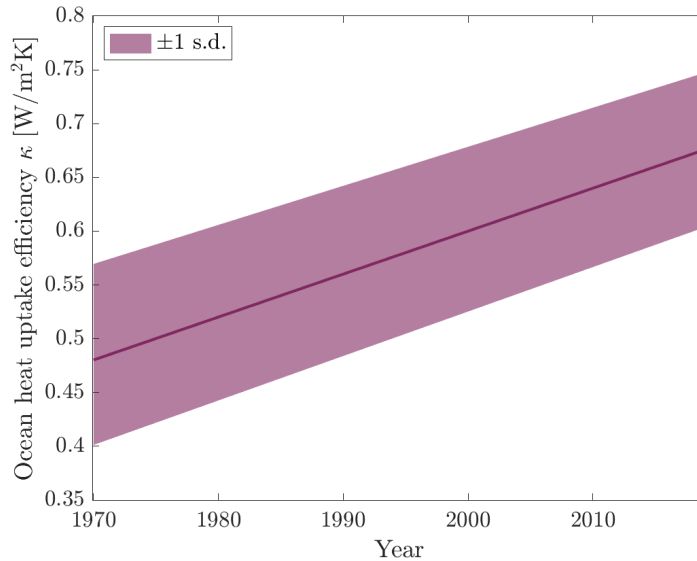


**Figure 3.** Ocean heat uptake efficiency  $\kappa$ , [W/m<sup>2</sup>K] vs. time.

113 spheric CO<sub>2</sub> increases by 1% a year, a  $\kappa$  like that diagnosed for 1970 results in the ex-  
 114 ceeding 1.5°C (2°C) warming by 5.0±1.2 years (6.7±1.5 years) earlier than a  $\kappa$  like that  
 115 diagnosed for 2019. While these calculations are based on the heuristic metric of TCS,  
 116 they still nonetheless underscore an appreciable evolution of  $\kappa$  diagnosed here in terms  
 117 of climate policy and projection. This difference will of course be even greater if the in-  
 118 crease in  $\kappa$  continues, with opposite implications if the trend reverses in the near future.  
 119 The numbers in this paragraph are intended to be illustrative of the implications of a  
 120 positive trend in OHUE; all are uncertain stemming from the similar uncertainty in  $\delta$ ,  
 121 and the sign of each of these holds with the same >99% confidence.

122 The likely increase in OHUE over the past five decades is attributed to the steep-  
 123 ening of anthropogenic heat gradients over this time period as anthropogenic heat is ac-  
 124 cumulated in the ocean. Heat is primarily stored in the ocean in i) the Southern Ocean  
 125 and ii) the North Atlantic Ocean due to the overturning circulation, and iii) via stirring  
 126 and mixing of gradients by eddies and other forms of ocean turbulence (Morrison et al.,  
 127 2013). The increase in OHUE cannot be due to the first two of these, principally because  
 128 the overturning circulation in neither the Southern Ocean nor the North Atlantic Ocean  
 129 has not yet shown a definite systemic strengthening over this time period in observations  
 130 (Meredith et al., 2012; Kilbourne et al., 2022). In contrast, the gradients of anthropogenic  
 131 heat in the ocean have steadily increased over this time period as heat is continually in-  
 132 jected into the upper ocean and comparatively slowly diffused into its interior (Cheng  
 133 et al., 2017; Cheng, 2022). Analogous to Fick’s first law of diffusion, the steeper the gra-  
 134 dients of anthropogenic heat, the more efficiently ocean turbulent processes can act to  
 135 transport heat away from the surface. This results in a larger OHUE, because every ad-  
 136 ditional amount of heat added to the surface ocean can be more easily transported into  
 137 the ocean interior as these gradients steepen. This is also visible in the increased frac-  
 138 tion of total OHC contained in deeper layers of the ocean over time (Cheng et al., 2017;  
 139 Cheng, 2022). The change in  $\kappa$  is thus a result of passive transport of heat by ocean dy-  
 140 namics, rather than by the direct influence of the injected heat on the ocean’s dynam-  
 141 ics. This also explains why the change in  $\kappa$  is better explained as a temporal evolution  
 142 than a temperature-dependent climate feedback, as its change is due to the steady steep-  
 143 ening of these gradients.

144 As this is a generic phenomenon, the increase in OHUE over time is expected to  
 145 continue in the near future, as anthropogenic heat gradients should continue to steepen  
 146 in the ocean. Note that no evidence for a reversal of this increasing trend is observable  
 147 in the residuals of the regression in Figure 1. However, it is important to note that this  
 148 multidecadal increase in  $\kappa$  is not in disagreement with the centennial-scale decrease in  
 149  $\kappa$  observed in ESMs, which is thought to be due to the equilibration of the deep ocean  
 150 with Earth’s surface, i.e. the eventual smoothing out of anthropogenic heat gradients  
 151 (Gregory et al., 2015; Watanabe et al., 2013) and may also be a response to future cir-  
 152 culation changes. Even under sustained radiative forcing, the deep ocean should even-  
 153 tually accumulate enough heat to weaken these anthropogenic heat gradients and OHUE  
 154 should therefore decrease, as found in ESM experiments. ESMs should however be able  
 155 to replicate this multidecadal increase in  $\kappa$ , though they are expected to reach an equi-  
 156 librium temperature (corresponding to the equilibrium climate sensitivity) at some point  
 157 after radiative forcing is stabilised. It is possible however that 140 years is too fast a timescale  
 158 to expect the deep ocean to equilibrate with Earth’s surface under sustained emissions.  
 159 It would be instructive to investigate the centennial  $\kappa$  behaviour within ESMs that can  
 160 resolve the multidecadal increasing trend in  $\kappa$  diagnosed from observations here. OHUE  
 161 may also decrease over time due to overturning circulation changes that have not yet oc-  
 162 curred.

163 Altogether these results demonstrate the importance of deriving observational es-  
 164 timates of the key climate parameters that determine the Earth’s response to anthro-  
 165 pogenic forcing, as well as the evolution of these parameters over time, as critical coun-  
 166 terpoints to ESM estimates both to evaluate models and to make independent projec-  
 167 tions. It would be most instructive to apply the method presented here to large ensem-  
 168 bles of historical simulations as an indicator of model performance. That said, the method  
 169 assumes a linear trend over the entire period, which is effective for finding an average  
 170 change over time and justified by the lack of curvature in the residuals, but necessarily  
 171 misses whether this trend may have reversed at some point or been confined to partic-  
 172 ular periods. Finally, the method presented here is a simple statistical diagnosis of changes  
 173 in, and time-mean, OHUE, relying only on surface temperature and ocean heat content  
 174 records; it therefore cannot distinguish how different forcing agents such as anthropogenic  
 175 aerosols or volcanic eruptions, nor different modes of climate variability such as the El  
 176 Niño Southern Oscillation, influence OHUE. It also cannot distinguish the extent to which  
 177 diagnosed trends are due to or modulated by natural climate variability. Understand-  
 178 ing the influence of such factors is an important part of utilising this observational di-  
 179 agnosis to evaluate ESMs.

### 180 3 Materials and Methods

181 **Theory:** The flux of energy from the Earth’s surface boundary layer into the ocean  
 182  $H$  [ZJ/year] can be integrated from an initial time point  $t_i$  to yield the ocean heat con-  
 183 tent anomaly  $\mathcal{H}(t)$  [ZJ]:

$$\mathcal{H}(t) = \int_{t_i}^t H(\tau) d\tau$$

184 where  $\tau$  is a dummy variable. The ocean heat content efficiency  $\kappa$  [ZJ/K y] is de-  
 185 fined as this energy flux per degree of global warming, i.e.  $\kappa = H/T$  so that

$$\mathcal{H}(t) = \int_{t_i}^t H(\tau) d\tau = \int_{t_i}^t \kappa(\tau)T(\tau) d\tau$$

186 The ansatz is then made that  $\kappa = \kappa_i(1 + \delta(t - t_i))$ , i.e.  $\kappa$  starts at  $\kappa_i$  at  $t_i$  and  
 187 increases by a constant amount  $\delta\kappa_i$  each year –  $\delta$  here is a number (in units of  $y^{-1}$ ), not

188 the Kronecker delta function. For simplicity  $t_i$  is redefined as year zero so  $\kappa = \kappa_i(1 +$   
 189  $\delta t)$ ; one can then substitute

$$\mathcal{H}(t) = \int_{t_i}^t \kappa_i(1 + \delta\tau)T(\tau) d\tau = \kappa_i \int_{t_i}^t (1 + \delta\tau)T(\tau) d\tau$$

190 The year 1970 is then redefined as the initial year and the initial ocean heat up-  
 191 take efficiency is labeled as  $\kappa_{1970}$  for clarity. If one then defines

$$\mathcal{T}_\delta(t) = \int_{t_i}^t (1 + \delta\tau)T(\tau) d\tau$$

192 then the slope

$$\mathcal{H}(t)/\mathcal{T}_\delta(t) = \kappa_{1970}$$

193 If the ansatz is valid and the correct  $\delta$  is selected, this  $\delta$  will capture all the time-  
 194 dependence of  $\kappa$  and this slope will be constant in time, i.e. there will be no systematic  
 195 behavior or curvature in the residuals of  $\mathcal{H}(t)$  regressed against  $\mathcal{T}_\delta(t)$ . Finally for all fig-  
 196 ures,  $\kappa$  is divided by a factor of 16.09 to convert zetajoules per degree Kelvin per year  
 197 to watts per square meter per second; this is the surface area of the Earth ( $5.101 \times 10^{14}$   
 198  $\text{m}^2$ ) times the number of seconds in a year ( $3.154 \times 10^7$ ) divided by the number of joules  
 199 in a zetajoule ( $10^{21}$ ). Note that this is an average over the full Earth surface, not just  
 200 the ocean surface, in keeping with the standard definition.

201 **Temperature data:** The HadCRUT5 temperature record is used here, which is  
 202 provided as a 200-member ensemble. From this ensemble a 10,000 member ensemble is  
 203 generated by calculating the estimated Gaussian covariance matrix based on the ensemble  
 204 and simulating 10,000 members with the same covariance properties as the original  
 205 ensemble. Repeating the analysis with the original 200-member ensemble yields effec-  
 206 tively identical results. HadCRUT5 is described in detail in (Morice et al., 2021).  $T(t)$   
 207 [K] is defined as the temperature anomaly versus the 1850-1900 average. This temper-  
 208 ature record is selected because i) uncertainties being expressed as ensemble members  
 209 makes the propagation of uncertainty straightforward when integrating in time, and ii)  
 210 the HadCRUT5 ensemble captures the uncertainty across temperature time series. Specif-  
 211 ically, when 0.03 K is subtracted from the  $T(t)$  ensemble, 99% of the temperatures across  
 212 all years of five other temperature products (Hersbach et al., 2020; Rohde & Hausfather,  
 213 2020; Cowtan & Way, 2014; Hansen et al., 2006; Lindsey & Dahlman, 2020) are above  
 214 (below) the 1st (99th) percentile of the ensemble. This value of 0.03 K is not subtracted  
 215 from the ensemble for the calculations herein, but subtracting it does not change the re-  
 216 sults.

217 **Ocean heat content data:** The Japanese Meteorological Agency, (JMA, 2022;  
 218 Ishii et al., 2017), Cheng (Cheng et al., 2017; Cheng, 2022), and National Centers for  
 219 Environmental Information (Domingues et al., 2008; Levitus et al., 2012) ocean heat con-  
 220 tent records are used here, which are provided as ocean heat content over 0-2000m. A  
 221 10,000 member ensemble is generated from these by calculating the estimated Gaussian  
 222 covariance matrix from the three time-series and simulating ensemble members with the  
 223 same covariance properties. The ensemble thus accounts for the across-product uncer-  
 224 tainties. The time series are described in detail in the above citations; the values were  
 225 taken from the links given in the Acknowledgments.  $\mathcal{H}(t)$  [ZJ] is defined as the ocean heat  
 226 content anomaly; the reference year is immaterial for the analysis here as only changes  
 227 over time affect the parameters. Reanalysis products are not considered because these  
 228 “are not suitable for studies of long-term trends or low frequency variability across data-  
 229 sparse time periods” (Killick & for Atmospheric Research Staff (Eds.), 12 June 2020).

Years from 1970 onwards are considered because i) ocean heat content changes are more sparsely observed and uncertain before this year, ii) changes in both ocean heat content and temperature are very small over the years that ocean heat content data are available in a subset of these products prior to this year compared to both this uncertainty and interannual variability, indicating there is little to no signal to extract, and iii) these are the years for which these three observational ocean heat content products are available for comparison to generate an across-product ensemble.

**Initial curvature calculation:** Time-evolution of  $\kappa$  (i.e.  $\delta \neq 0$ ) is tested for initially by regressing  $\mathcal{H}(t)$  versus each ensemble member of  $\mathcal{T}_{\delta=0}(t)$ . A quadratic regression is performed. For >99% of these regressions the quadratic term is positive, indicating that  $\delta$  is significantly positive and necessary to describe the relationship between  $T$  and  $\mathcal{H}$ .

**Primary analysis:** To generate an estimate of  $\kappa_{1970}$  and  $\delta$ , for each  $T(t)$  ensemble member, the following procedure is followed: i) sample a large range of  $\delta$  values (in practice the range  $-0.005$  to  $0.02 \text{ y}^{-1}$  at  $0.0001$  resolution is sufficient; see Figure 2), ii) calculate  $\mathcal{T}_{\delta}(t)$  for each, iii) perform a linear regression of  $\mathcal{H}(t)$  against  $\mathcal{T}_{\delta}(t)$  for each, iv) select the  $\delta$  value for which the linear regression has the lowest residual sum of squares (or equivalently the highest  $r^2$  or equivalently the lowest root-mean-square error). The associated  $\kappa_{1970}$  is the slope of this  $\delta$ 's linear regression (Figure 1). These  $\delta$  values yielded linear relationships between  $\mathcal{H}(t)$  and  $\mathcal{T}_{\delta}(t)$ ; the quadratic term in a quadratic regression analogous to that described for the  $\delta = 0$  case was  $<1z$ -score different from zero for all ensemble members.

**Temperature vs. time analysis:** The evolution of  $\kappa$  as a function of time is compared to that of a temperature-dependent  $\kappa$ , i.e. the ansatz  $\kappa = \kappa_{1970}(1 + \delta T)$  is compared to the ansatz  $\kappa = \kappa_{1970}(1 + \delta t)$  in the main text. A temperature-dependent  $\kappa$  would correspond to a type of temperature-dependent climate feedback, whereby the climate sensitivity depends on the temperature itself (Bloch-Johnson et al., 2021). The above analysis is repeated with the alternative ansatz to evaluate which model has the higher  $r^2$  (or equivalently the lower residual sum of squares or equivalently the lower root-mean-square error); in 82%% instances this is the time-dependent model, indicating the ansatz in the text is a better description of the evolution of  $\kappa$  than a temperature-dependent  $\kappa$ .

**Years to 1.5 or 2°C:** To estimate the difference in years taken to surpass  $1.5^\circ\text{C}$  or  $2^\circ\text{C}$ , the transient climate sensitivity  $TCS = F_{2\times\text{CO}_2}/(-\lambda + \kappa)$  is calculated, where  $F_{2\times\text{CO}_2} = N(4.0, 0.3) \text{ W/m}^2$  is the radiative forcing associated with a doubling of  $\text{CO}_2$  and  $\lambda = N(-1.3, 0.44) \text{ W/m}^2\text{K}$  is the climate feedback (Sherwood et al., 2020). Note that the TCS is closely related to the arguably more relevant metric of the transient climate response (Winton et al., 2010); the TCS is preferred in this context, however, as the TCR would require a specification of the surface boundary layer's heat capacity, a term that is less certain than those that comprise the TCS. The TCS analysis is equivalent to TCR under the plausible assumption that the surface boundary layer's heat capacity is on the order of 30 ZJ or less, equivalent to roughly the top 10m of the global ocean. The year of crossing a temperature threshold of  $C$  degrees is then defined as  $y = 70C/TCS$ ; 70 is the number of years that is required for atmospheric  $\text{CO}_2$  concentrations to increase at 1% per year until the concentration doubles, which corresponds to a linear increase in radiative forcing under the assumption of logarithmic  $\text{CO}_2$  forcing (Bloch-Johnson et al., 2021). For each  $(\kappa_{1970}, \delta)$  pair, a random value of  $F_{2\times\text{CO}_2}$  and  $\lambda$  are sampled from the distributions above, and  $y$  is calculated for  $C = 1.5$  and  $2^\circ\text{C}$ , and for  $\kappa_{1970}$  and  $\kappa_{2019} = \kappa_{1970}(1 + 49\delta)$ . The difference  $y(C = 2, \kappa_{2019}) - y(C = 2, \kappa_{1970})$  is  $6.7 \pm 1.5$  years; the difference  $y(C = 1.5, \kappa_{2019}) - y(C = 1.5, \kappa_{1970})$  is  $5.0 \pm 1.2$  years. Note that this is a heuristic metric and is only intended to illustrate the potential impact of the change in  $\kappa$  diagnosed herein. It is emphasised that no extrapolation of the

282 observed trend is used here; only the initial and final  $\kappa$  values are compared, and are ap-  
 283 plied as time-invariant quantities.

## 284 Acknowledgments

285 It is a pleasure to thank the many scientists whose collective work has generated the time  
 286 series on which this work relies. This work was support by the European Union’s Hori-  
 287 zon 2020 Research and Innovation Programme under grant agreement No. 820989 (project  
 288 COMFORT). The work reflects only the authors’ view; the European Commission and  
 289 their executive agency are not responsible for any use that may be made of the infor-  
 290 mation the work contains. Cael conceived the study, performed the analyses, and wrote  
 291 the paper. The author has no competing interests to declare. **Open Research:** The data  
 292 on which this article is based are available at [https://www.metoffice.gov.uk/hadobs/  
 293 hadcrut5/data/current/download.html](https://www.metoffice.gov.uk/hadobs/hadcrut5/data/current/download.html), [https://www.data.jma.go.jp/gmd/kaiyou/  
 294 english/ohc/ohc\\_en\\_data\\_en.html](https://www.data.jma.go.jp/gmd/kaiyou/english/ohc/ohc_en_data_en.html), <http://159.226.119.60/cheng/>, and [https://  
 295 www.ncei.noaa.gov/access/global-ocean-heat-content/index.html](https://www.ncei.noaa.gov/access/global-ocean-heat-content/index.html). Code is avail-  
 296 able for review purposes at [github.com/bbcael/ohue](https://github.com/bbcael/ohue) and will be deposited to a FAIR com-  
 297 pliant repository if this article is eventually accepted.

## 298 References

- 299 *Adoption of the Paris Agreement FCCC/CP/2015/L.9/Rev.1.* (2015). UNFCCC.
- 300 Armour, K. C., Bitz, C. M., & Roe, G. H. (2013). Time-varying climate sensitivity  
 301 from regional feedbacks. *Journal of Climate*, *26*(13), 4518–4534.
- 302 Bloch-Johnson, J., Rugenstein, M., Stolpe, M. B., Rohrschneider, T., Zheng, Y., &  
 303 Gregory, J. M. (2021). Climate sensitivity increases under higher co2 levels  
 304 due to feedback temperature dependence. *Geophysical Research Letters*, *48*(4),  
 305 e2020GL089074.
- 306 Cheng, L. (2022). *OHC by IAP*. <http://159.226.119.60/cheng/>. ([Online; ac-  
 307 cessed 7-April-2022])
- 308 Cheng, L., Trenberth, K. E., Fasullo, J., Boyer, T., Abraham, J., & Zhu, J. (2017).  
 309 Improved estimates of ocean heat content from 1960 to 2015. *Science Ad-  
 310 vances*, *3*(3), e1601545.
- 311 Cowtan, K., & Way, R. G. (2014). Coverage bias in the hadcrut4 temperature series  
 312 and its impact on recent temperature trends. *Quarterly Journal of the Royal  
 313 Meteorological Society*, *140*(683), 1935–1944.
- 314 Domingues, C. M., Church, J. A., White, N. J., Gleckler, P. J., Wijffels, S. E.,  
 315 Barker, P. M., & Dunn, J. R. (2008). Improved estimates of upper-ocean  
 316 warming and multi-decadal sea-level rise. *Nature*, *453*(7198), 1090–1093.
- 317 Gregory, J. M., Andrews, T., & Good, P. (2015). The inconstancy of the transient  
 318 climate response parameter under increasing co2. *Philosophical Transactions  
 319 of the Royal Society A: Mathematical, Physical and Engineering Sciences*,  
 320 *373*(2054), 20140417.
- 321 Gregory, J. M., & Mitchell, J. F. (1997). The climate response to co2 of the hadley  
 322 centre coupled aogcm with and without flux adjustment. *Geophysical Research  
 323 Letters*, *24*(15), 1943–1946.
- 324 Hansen, J., Ruedy, R., Sato, M., & Lo, K. (2006). Nasa giss surface temperature  
 325 (gistemp) analysis. *Trends: A Compendium of Data on Global Change*.
- 326 Hersbach, H., Bell, B., Berrisford, P., Hirahara, S., Horányi, A., Muñoz-Sabater, J.,  
 327 ... others (2020). The era5 global reanalysis. *Quarterly Journal of the Royal  
 328 Meteorological Society*, *146*(730), 1999–2049.
- 329 Ishii, M., Fukuda, Y., Hirahara, S., Yasui, S., Suzuki, T., & Sato, K. (2017). Ac-  
 330 curacy of global upper ocean heat content estimation expected from present  
 331 observational data sets. *Sola*, *13*, 163–167.

- 332 JMA. (2022). *JMA's global ocean heat content data*. [https://www.data.jma.go.jp/gmd/kaiyou/english/ohc/ohc\\_data\\_en.html](https://www.data.jma.go.jp/gmd/kaiyou/english/ohc/ohc_data_en.html). ([Online; accessed 7-April-2022])
- 333  
334
- 335 Kilbourne, K. H., Wanamaker, A. D., Moffa-Sanchez, P., Reynolds, D. J., Amrhein,  
336 D. E., Butler, P. G., ... others (2022). Atlantic circulation change still uncertain. *Nature Geoscience*, *15*(3), 165–167.
- 337
- 338 Killick, R., & for Atmospheric Research Staff (Eds.), N. C. (12 June 2020).  
339 *The Climate Data Guide: EN4 subsurface temperature and salinity for the*  
340 *global oceans*. <https://climatedataguide.ucar.edu/climate-data/en4-subsurface-temperature-and-salinity-global-oceans>. ([Online; accessed 7-April-2022])
- 341  
342
- 343 Kuhlbrodt, T., & Gregory, J. (2012). Ocean heat uptake and its consequences for  
344 the magnitude of sea level rise and climate change. *Geophysical Research Letters*,  
345 *39*(18).
- 346 Levitus, S., Antonov, J. I., Boyer, T. P., Baranova, O. K., Garcia, H. E., Locarnini,  
347 R. A., ... others (2012). World ocean heat content and thermosteric sea level  
348 change (0–2000 m), 1955–2010. *Geophysical Research Letters*, *39*(10).
- 349 Lindsey, R., & Dahlman, L. (2020). Climate change: Global temperature. *Climate*.  
350 *gov*, *16*.
- 351 Meredith, M. P., Naveira Garabato, A. C., Hogg, A. M., & Farneti, R. (2012). Sen-  
352 sitivity of the overturning circulation in the southern ocean to decadal changes  
353 in wind forcing. *Journal of Climate*, *25*(1), 99–110.
- 354 Morice, C. P., Kennedy, J. J., Rayner, N. A., Winn, J., Hogan, E., Killick, R., ...  
355 Simpson, I. (2021). An updated assessment of near-surface temperature  
356 change from 1850: The hadcrut5 data set. *Journal of Geophysical Research:*  
357 *Atmospheres*, *126*(3), e2019JD032361.
- 358 Morrison, A., Saenko, O., Hogg, A. M., & Spence, P. (2013). The role of vertical  
359 eddy flux in southern ocean heat uptake. *Geophysical Research Letters*, *40*(20),  
360 5445–5450.
- 361 Newsom, E., Zanna, L., Khatiwala, S., & Gregory, J. M. (2020). The influence of  
362 warming patterns on passive ocean heat uptake. *Geophysical Research Letters*,  
363 *47*(18), e2020GL088429.
- 364 Padilla, L. E., Vallis, G. K., & Rowley, C. W. (2011). Probabilistic estimates of  
365 transient climate sensitivity subject to uncertainty in forcing and natural vari-  
366 ability. *Journal of Climate*, *24*(21), 5521–5537.
- 367 Raper, S. C., Gregory, J. M., & Stouffer, R. J. (2002). The role of climate sensitiv-  
368 ity and ocean heat uptake on aogcm transient temperature response. *Journal*  
369 *of Climate*, *15*(1), 124–130.
- 370 Rohde, R. A., & Hausfather, Z. (2020). The berkeley earth land/ocean temperature  
371 record. *Earth System Science Data*, *12*(4), 3469–3479.
- 372 Rose, B. E., Armour, K. C., Battisti, D. S., Feldl, N., & Koll, D. D. (2014). The de-  
373 pendence of transient climate sensitivity and radiative feedbacks on the spatial  
374 pattern of ocean heat uptake. *Geophysical Research Letters*, *41*(3), 1071–1078.
- 375 Sellers, W. D. (1969). A global climatic model based on the energy balance of the  
376 earth-atmosphere system. *Journal of Applied Meteorology and Climatology*,  
377 *8*(3), 392–400.
- 378 Sherwood, S., Webb, M. J., Annan, J. D., Armour, K. C., Forster, P. M., Harg-  
379 reaves, J. C., ... others (2020). An assessment of earth's climate sensitivity us-  
380 ing multiple lines of evidence. *Reviews of Geophysics*, *58*(4), e2019RG000678.
- 381 Watanabe, M., Kamae, Y., Yoshimori, M., Oka, A., Sato, M., Ishii, M., ... Kimoto,  
382 M. (2013). Strengthening of ocean heat uptake efficiency associated with the  
383 recent climate hiatus. *Geophysical Research Letters*, *40*(12), 3175–3179.
- 384 Winton, M., Takahashi, K., & Held, I. M. (2010). Importance of ocean heat uptake  
385 efficacy to transient climate change. *Journal of Climate*, *23*(9), 2333–2344.